PHILOSOPHICAL TRANSACTIONS OF THE ROYAL SOCIETY A MATHEMATICAL, PHYSICAL & ENGINEERING SCIENCES

NMR Imaging of Fluids in Porous Solids [and Discussion]

P. A. Osment, K. J. Packer, M. J. Taylor, J. J. Attard, T. A. Carpenter, L. D. Hall, N. J. Herrod, S. J. Doran, R. F. Gordon, K. J. Packer, E. L. Hahn, E. R. Andrew, P. A. Bottomley, I. R. Young, A. N. Garroway, J. Frahm and E. W. Randall

Phil. Trans. R. Soc. Lond. A 1990 **333**, 441-452
doi: 10.1098/rsta.1990.0171

NMR imaging of fluids in porous solids

By P. A. Osment[1], K. J. Packer[1], M. J. Taylor[1], J. J. Attard[2], T. A. Carpenter[2], L. D. Hall[2], N. J. Herrod[2] and S. J. Doran[2]

[1] *BP Research, Research Centre Sunbury, Chertsey Road, Sunbury-on-Thames, Middlesex TW16 7LN, U.K.*

[2] *Herchel Smith Laboratory for Medicinal Chemistry, University Forvie Site, Robinson Way, Cambridge CB2 2PZ, U.K.*

The principles governing the NMR behaviour of ^{1}H-containing fluids permeating porous solids, such as hydrocarbon reservoir rocks, are outlined. The additional capabilities of NMR imaging methods for characterizing these systems is considered. Experimental results are presented for NMR imaging applied to a model porous solid (alumina) and natural sandstone and limestone rocks, saturated with aqueous phases. Both three-dimensional and slice-selected two-dimensional FT spin echo methods are used and the images demonstrate the capability of NMRI in these systems to reveal internal structures of the porous solids. Simple strategies for characterizing the spatial heterogeneity of these materials in terms of histograms and correlation functions are proposed and a general pixel fitting program is used to examine some of the data in terms of such histograms and related property maps.

1. Introduction

The imaging by NMR of solids, in which the NMR linewidth is dominated by secular interactions, requires special techniques as discussed by Garroway and Strange (this symposium). In the case of porous solids, however, the possibility exists of imaging the void space, and hence indirectly the solid, through the NMR signal of fluids permeating the structure. For the particular case of aqueous and hydrocarbon phases contained in their natural reservoir rocks, these contained fluids, and their interactions with the rock structure and each other, are of importance in hydrocarbon resource recovery. Given that NMRI may generate image contrast through spin density, chemical shift, spin relaxation behaviour and fluid transport properties it should be an extremely powerful method for characterizing and quantifying the properties of the fluid–rock systems and the processes involved in the movement of the fluids relative to the porous rock. It has the additional attraction that these investigations can, if required, be carried out under conditions of temperature, pressure, fluid flow rate, etc., characteristic of reservoir conditions. Despite this seemingly favourable coincidence between experimental capability and opportunity there are only a handful of substantive reports of work in this area (see for example, Rothwell & Vinegar 1985; Vinegar 1986; Blackband *et al.* 1986; Hall & Rajanayagam 1986; Edelstein *et al.* 1988; Baldwin & Yamanashi 1988; Horsfield *et al.* 1989). The main reasons for this are the fact that the development drive in NMRI has been largely medical with the consequence that the instrumental specifications do not necessarily match those required for applications to materials problems, and the associated high cost of this instrumentation. The constraints placed on commercial NMRI hardware

by the requirements of living subjects are clearly not relevant to inanimate samples and the NMR properties of fluids in such rocks may require performance specifications beyond those generally available from medical NMRI systems (Edelstein *et al.* 1988).

In NMR terms there is no difference, qualitatively, between biological systems, which have been studied extensively with NMRI methods, and the type of systems of concern here. They each comprise heterogeneous 'solid' structures, on scales from molecular to macroscopic, with more mobile 'liquid' phases permeating and interacting with the 'solids'. These latter are connective tissue, bone, cell membranes, etc., in the biological systems and are quartz minerals, limestones, clays, etc., in the case of oil reservoir rocks. The principal differences are of degree. The mobile 'liquid' content is usually much higher in the biological materials and the effects of the 'solids' on the spin relaxation properties of the 'liquids' weaker. Both of these factors make imaging in biological materials somewhat easier in general.

In this paper we review (§2) the factors influencing the NMR properties of spins in fluids contained in porous solids and consider the implications for NMRI in such systems. In addition, the question of spatial heterogeneity is addressed. The remaining sections give experimental details and results of preliminary NMRI investigations of a number of porous solids saturated with water or brine.

2. NMR in porous solids

(*a*) *General*

Typically, in a porous solid, the pore space will have a complex topology, particularly if it is of natural origin. The local scale of the pore space may be represented by a 'radius' a. There will often be a distribution of such scales in any real sample, the statistics of this distribution being of interest both in terms of its overall properties and its spatial organization. There will be differences in magnetic susceptibility between the fluids permeating the pore space, the solid matrix and also the whole sample and its environment, and these can have significant effects on the NMR behaviour of contained fluids. The principal effects of the solid matrix on these NMR properties arise through enhanced relaxation of the fluid spins at the walls of the pore space, gradients in the local values of the magnetic field arising from differences in magnetic susceptibility and the effects of diffusion of the spin-bearing molecules within the pore space. The ability to carry out an NMRI characterization of such a system will depend, *inter alia*, on the range of both spin-lattice and transverse relaxation times it exhibits, the resolution required, the imaging gradients available, the spectrometer bandwidth and the degree to which quantitative information is required.

Spin-lattice relaxation of aqueous brine in sandstone rocks has been studied extensively (see, for example, Kenyon *et al.* 1988). The relationship between spin-lattice relaxation behaviour and the scale of the pore space, the diffusion of the fluid molecules and the effectiveness of the pore surface in relaxing the spins can be described in detail for regular geometries (Brownstein & Tarr 1979). Neglecting the detail of the geometry the behaviour is characterized by the two limiting régimes of 'fast diffusion' (single exponential relaxation for each pore with T_1 proportional to the 'radius') and 'slow diffusion' (multiple exponential relaxation with the dominant longest T_1 proportional to the 'radius' squared).

In any real rock there is a distribution of pore sizes $P(a)$ and the observed strongly non-single exponential relaxation behaviour may be inverted to yield $P(a)$ (see, for

PHILOSOPHICAL TRANSACTIONS OF THE ROYAL SOCIETY A MATHEMATICAL, PHYSICAL & ENGINEERING SCIENCES

example, Davies & Packer 1990; Davies *et al.* 1990). A significant question for NMRI is at what resolution is the $P(a)$ representative and is the surface-induced relaxation strength homogeneously distributed?

Transverse relaxation has similar contributions from the effects of surface relaxation although with different values of the surface relaxation strength. Observations of transverse relaxation of brine-saturated porous sandstone rocks using Carr–Purcell/Gill–Meiboom (CPMG) multiple spin echo sequences (Bendel 1990; Kleinberg & Horsfield 1990) show that, in general, the relaxation is multiple exponential, is faster than the corresponding spin-lattice relaxation, lengthens as the pulse spacing in the CPMG sequence is reduced, and shortens with increasing applied field. These observations are indicative of significant contributions from diffusion of the molecules through locally inhomogeneous magnetic fields, these arising from the differences in magnetic susceptibility of the rock matrix and contained fluid and reflecting the geometry of the pore space.

In a system containing two, or more, immiscible fluid phases, the same general principles apply. However, the accessibility of the pore surface to the different phases will depend on the relative wetting capabilities and the details of how the saturation was achieved. In a strongly water wet system it is likely, for example, that the influence of the rock surface on the relaxation of a contained hydrocarbon phase will be small. The ability of an NMR measurement to characterize separately aqueous and hydrocarbon phases will depend on the details of these effects. Strong broadening of ^{1}H resonance lines by magnetic susceptibility difference/diffusion will make chemical shift discrimination difficult but differential T_1/T_2 effects can allow separate characterization of these phases. If necessary, discrimination can be induced by the use of deuterated or paramagnetically doped phases.

A further point to be considered is that most fluid-saturated rock samples are electrically conducting. This means that care must be taken to ensure that differential effects on coil loading, tuning and matching and RF penetration must be taken into account, particularly for quantitative measurements.

The significance of this underlying physics of relaxation for quantitative NMRI measurements depends on the particular methods used. However, the use of spin echoes, which is almost universal, involves T_2 and, often, T_1 effects and, for example, reconstruction of a true M_0 image representing porosity can require accurate extrapolation of data to zero time, particularly if relaxation times are short (Edelstein *et al.* 1988). The acquisition of a suitable data set may be demanding on time if the dynamic range of the relaxation processes is large, which it often is, and for transverse relaxation the requirements may exceed the capability of the instrumental specifications in terms of the amplitude of gradients demanded, their switching times and the signal digitization rate needed.

(*b*) *Imaging*

For natural materials, such as hydrocarbon reservoir rocks, the available samples are normally derived from cores obtained from limited locations in the whole formation. As such, they already represent, in some sense, a spatially resolved view of the properties of interest. However, assuming that the ultimate control on fluid behaviour in these systems lies at the pore scale it is important to ask what extra information is provided by NMRI, how it should be represented and, finally, what is its significance? We address, here, the first two of these questions in a preliminary fashion.

PHILOSOPHICAL TRANSACTIONS OF THE ROYAL SOCIETY A MATHEMATICAL, PHYSICAL & ENGINEERING SCIENCES

The maximum spatial resolution which it is practical to use in NMRI of these systems is usually dictated by considerations of signal-to-noise (S/N) and the time required for the experiment. Typically, this highest resolution will be a voxel of the order of 0.05–0.2 μl with dimensions $0.2 \times 0.2 \times (1\text{–}5)$ mm^3. For most rocks the maximum scale of pores is somewhat less than the in-slice resolution of 0.2 mm, although in limestones voids larger than this do occur. In general then the voxel NMR properties are a superposition of those arising from a distribution of pore sizes, $p(a)$. This voxel pore size distribution (PSD) is a subset of the total PSD for the sample, $P(a)$, in the limit being identical with it. The simplest case to consider is saturation of the solid with a single fluid and we restrict our attention to that case. In addition, we restrict our attention to just two NMR properties, signal intensity and spin-lattice relaxation (SLR), although the discussion which follows could apply generally.

An NMRI data-set might give values for signal intensity, I_i, and SLR behaviour, $\Delta M_{zi}(t)$, for each voxel i. The intensity I_i is proportional to the porosity within voxel i and the mean value of the set $\{I_i\}$ gives the overall porosity when suitably calibrated (Edelstein *et al.* 1988). The extra information provided by NMRI is the spatial variation of this, and other, properties, for a given voxel size. This spatial variation may be characterized in a number of ways. A simple distribution or histogram can be generated and characterized in terms of those of its moments which are significant above the noise level. This discriminates samples in terms of their overall heterogeneity at a given image resolution. A more detailed characterization would be in terms of the spatial correlations of the property. A spatial correlation function of $I(\boldsymbol{r})$ could be defined as

$$g_I(\boldsymbol{r}) = N^{-1} \sum_{i=1}^{N} \left\{ \sum_{j=1}^{n_j} n_j^{-1} \left[\frac{I_i \cdot I_j(r_{ij})}{I_i^2} \right] \right\},$$

where the summation over j includes all successive shells of n_j voxels at distance r_{ij} from voxel i. At a given image resolution $g_I(r)$ will characterize the scale over which the porosity is correlated.

The SLR function, ΔM_{zi}, for each voxel will again reflect $p_i(a)$ and, in principle, could be inverted to estimate $p_i(a)$. However, achievable S/N in reasonable measurement times will generally make it impractical to take this approach. Characterization of the SLR in terms of either a small, fixed, number of exponential components or a stretched exponential is probably the optimal approach.

The set $\{T_{1i}\}$ can be treated as described above for $\{I_i\}$. However, there is additional information in the two sets together. This can be seen by realizing that, for example, a particular I_i value could arise from a number of different $p_i(a)$s. The T_{1i} values on the other hand provide information on pore size and, as such, the relationship between I_i and T_{1i} values should identify how strongly porosity at a given voxel resolution is correlated with pore size.

3. Experimental

(a) *Samples*

Three samples provided the results presented in this paper. These are a porous alumina, a sandstone from the Ninian field and a limestone from the Dukhan reservoir. All samples were cylindrical (4 cm diameter, 8 cm length) and, in the case of the rocks, were cut from 10 cm diameter cores. The natural samples were cleaned

PHILOSOPHICAL TRANSACTIONS OF THE ROYAL SOCIETY A MATHEMATICAL, PHYSICAL & ENGINEERING SCIENCES

by successive solvent extraction with toluene and methanol. The alumina sample was used as received. All samples were finally saturated under a pressure of 60 bar (6 MPa) for three days, the alumina with deionized water, the rocks with 3% NaCl brine. All samples were wrapped in polyester film to reduce fluid loss once saturated.

(*b*) NMR imaging

All ^{1}H NMR images were obtained with an Oxford Research Systems BIOSPEC 1 system operating at 83.7 MHz. A single turn, inductively coupled, transverse resonator, 9 cm × 4 cm diameter, produced 90° pulse lengths of 30–50 μs. The imaging gradients were generated using a home-built coil set with a diameter of 30 cm. All images were produced with Fourier transform spin echo methods, the three-dimensional data-set using two-phase encoding gradients. Two-dimensional data-sets were obtained by using slice selection together with one phase encode gradient. T_1-weighted images were obtained by using a saturation-recovery sequence followed by the usual two-dimensional imaging procedure. Details of each experiment are given in the relevant figure captions.

(*c*) *Data processing*

Images were generated using the commercial Fourier transform software on the spectrometer with further processing carried out on a local networked system using specialized programs. In particular, a program, PIXFIT, has been written to fit the data from relaxation-weighted image sets to characterize the relaxation behaviour and signal intensity of pixels. The program allows the selection of a threshold intensity below which a pixel is disregarded, a variety of relaxation functions (e.g. single, multiple or stretched exponentials) for fitting and the generation of both histogram and image representations of the fitted data. Typically the fitting of 32 128 × 128 relaxation-weighted images to a single exponential takes about 5 min.

4. Results and discussion

Figure 1*a* is a view of the three-dimensional ^{1}H image of the brine-saturated sandstone sample. An image processing program, using ray-casting techniques, has been used to generate this cut-away view with both longitudinal and transverse sections revealed. The image shows a well-defined and complex heterogeneity traversing a considerable length of the sample. The lack of signal which generates the contrast for this feature could arise from either a low porosity or an enhanced transverse relaxation rate. The feature is in fact a shale band and has a strongly reduced T_2 which dominates the reduction in signal. The complex structure of this band and the detail which can be revealed is illustrated also in figure 1*b* which is a slice-selected two-dimensional image of the same sample. The spatial resolution in these images is approximately $(300\ \mu m)^3$ for figure 1*a* and $(200\ \mu m)^2 \times 5$ mm for figure 1*b*.

Figure 2 is a transverse slice-selected image of the limestone sample. In this material there are occasional large voids (vugs), which can be significantly larger than the image resolution and which can then be identified and characterized by following them through successive slices. It can be seen that considerable details of the variation in fluid-filled porosity may be distinguished in such images. In general, limestones have somewhat longer relaxation times than sandstones and are, thus, often rather less demanding on spectrometer specifications. It is important to

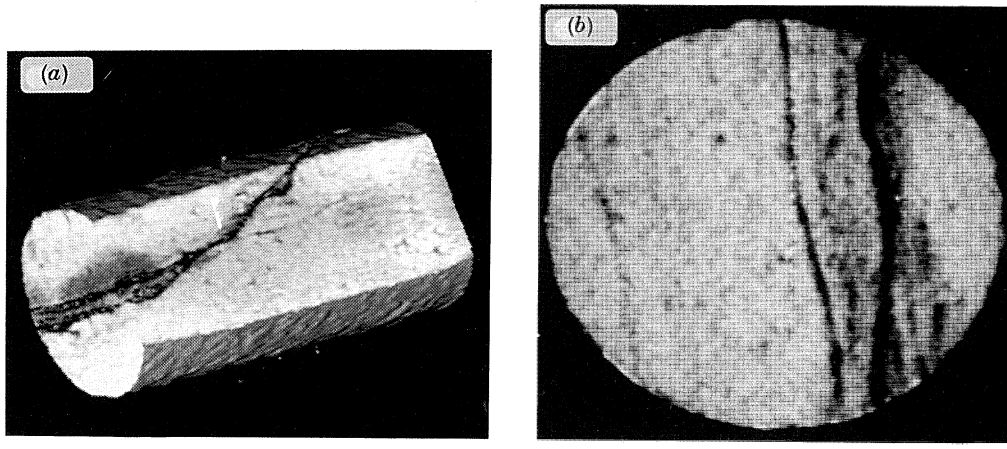

Figure 1. (*a*) A ^{1}H NMR image of the brine-saturated Ninian sandstone sample. The particular image displayed was selected from a full three-dimensional data-set [$z(128)$; $y(128)$; $x(256)$; voxel size $(300\ \mu m)^3$] processed using software based on ray-casting methods. The selection of cut-away sections was made to reveal the detail of the shale band traversing the sample. A single echo was acquired for each gradient combination with an echo time of 10 ms, a recycle time of 2 s and a dwell time of 6 μs. (*b*) A transverse slice-selected ^{1}H NMR image of the same sample. The in-plane resolution is 200 μm × 200 μm with a slice thickness of 5 mm.

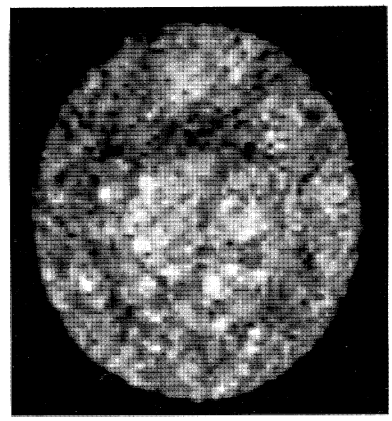

Figure 2. A transverse slice-selected (5 mm) ^{1}H NMR image of the brine-saturated Dukhan limestone sample. The data were obtained using an echo time of 4.6 ms, a recycle time of 16 s and a dwell time of 5 μs. The in-plane resolution is 300 μm × 300 μm.

recognize that the images presented here, although predominantly based on spin density, inevitably have some T_2 contrast incorporated. Only the use of the very shortest echo times can approach a true spin-density image and, even then, with echo times of the order of 1–2 ms, those regions with the smaller pore sizes are likely to be affected to some extent by T_2 contributions from diffusion through local field gradients. Under these circumstances only a careful characterization of the overall T_2 behaviour and extrapolation of a number of images taken with different echo times can lead to accurate intensity images.

Figure 3 summarizes, in the form of histograms, the results of analysis of ^{1}H NMR images of the alumina and Dukhan limestone samples using the PIXFIT program. The intensity histograms and images (see figure 4) are subject to effects of T_2 weighting

PHILOSOPHICAL TRANSACTIONS OF THE ROYAL SOCIETY A MATHEMATICAL, PHYSICAL & ENGINEERING SCIENCES

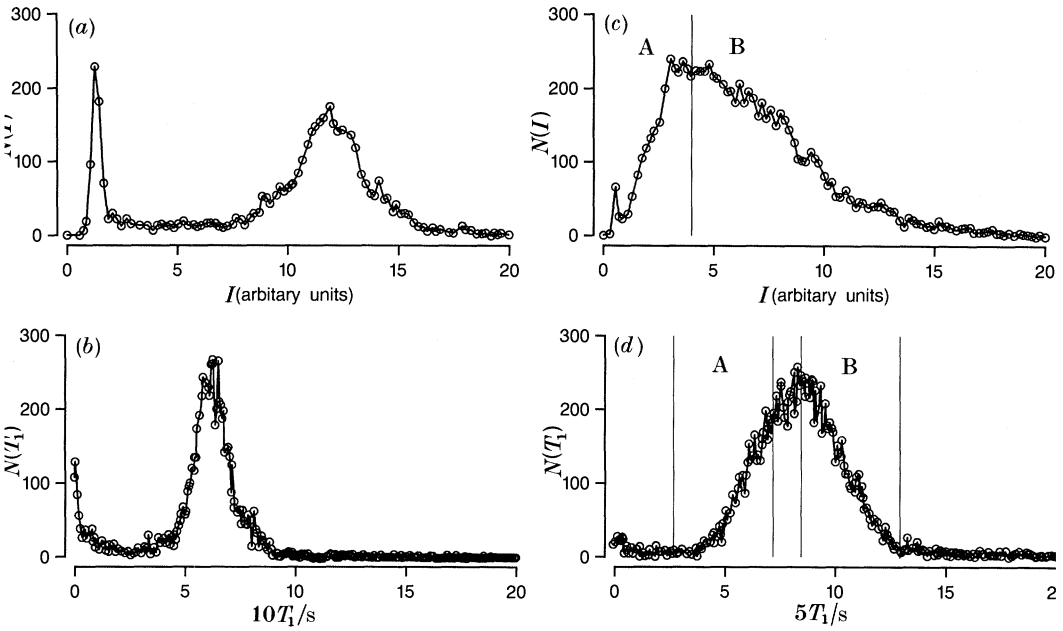

Figure 3. Intensity ((*a*) and (*c*)) and T_1 ((*b*) and (*d*)) histograms derived from the ^{1}H NMR images of the water-saturated alumina ((*a*) and (*b*)) and brine-saturated limestone ((*c*) and (*d*)) samples. The intensity data are not displayed on an absolute scale and contain effects of transverse relaxation. The T_1 and intensity values derive from a fit of each pixel relaxation to a single exponential process. The relaxation-weighted images were obtained using a saturation-recovery preparation followed by a slice-selected two-dimensional FT spin-echo imaging sequence. Each data-set comprised 128×128 pixel images (slice thickness 5 mm) for each of 32 SLR recovery times in the range 50–1600 ms. Read and maximum phase-encode gradients were 6000 Hz cm^{-1} for the alumina and 1600 Hz cm^{-1} for the Dukhan samples with echo times of 6.65 and 15.9 ms respectively. Single transients were acquired for each parameter set and the number and separation of the saturation pulses were 9 and 5 ms and 6 and 20 ms for alumina and Dukhan. Regions labelled A and B delineate the ranges used to generate figure 4*a*, *b*.

as discussed above. In addition, the samples had been allowed to partly dry (alumina) and drain (Dukhan) before these measurements were taken. Figure 3*a* shows a bimodal distribution of signal intensity for the partly dried alumina sample, and an image, constructed only from those pixels which form the low intensity feature, revealed that these lie almost exclusively at the periphery of the cylindrical sample, consistent with the partial drying out. The T_1 histogram of this sample, figure 3*b*, is, however, monotonic and rather narrow, with a width which is probably dominated by noise. Despite this and the lack of a bimodal structure, a full range T_1 image showed that the shorter relaxation times are distributed around the edge of the sample and to one side. Figure 3*c*, *d* shows the corresponding histograms for the Dukhan sample. It is clear, immediately, that this sample is more heterogeneous than the alumina, both histograms being much broader. Figure 4 shows images of the Dukhan sample which illustrate the spatial character associated with the histograms of figure 3*c*, *d*. Figure 4*a*, *b* shows two-level images of intensity and T_1, respectively, the ranges selected indicated on the histograms figure 3*c*, *d*. These images show clearly the draining of the sample that had taken place and the consequent gradients in fluid distribution (figure 4*a*). Close comparison of 4*a* and 4*b* shows some differences between the intensity and T_1 images with, for example, some longer T_1 pixels

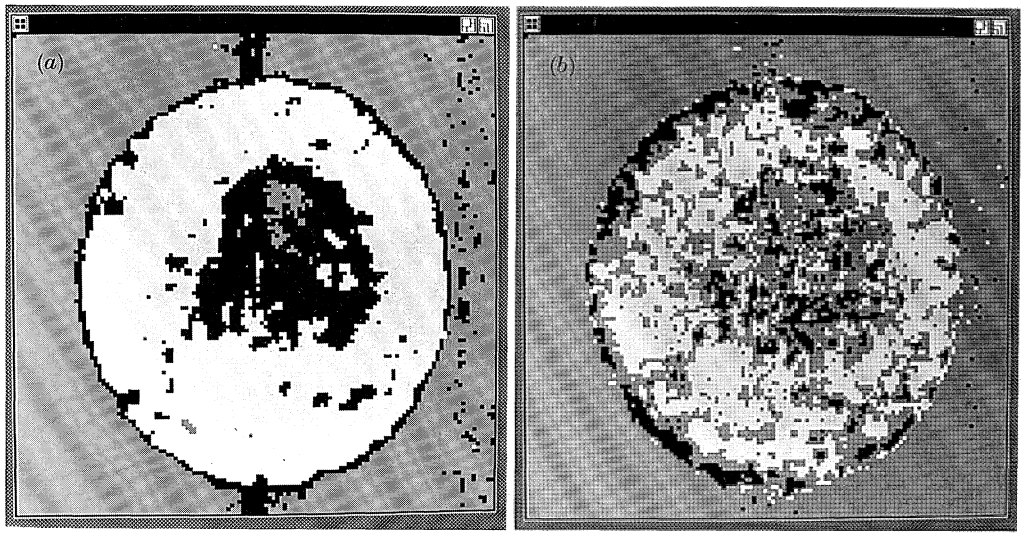

Figure 4. Image displays of the Dukhan data shown in figure 3. These are two-level (black and white) intensity and T_1 maps, (*a*) and (*b*) respectively, corresponding to the ranges identified in figure 3*c*, *d*, with black representing range A and white range B. Grey pixels are those excluded on the basis that they contain below the set threshold intensity and those which were unable to be fitted, for whatever reason.

occurring in the region assigned the lower intensity. These could be influenced by the particular choice of parameter ranges used to generate the image but could also suggest the need to investigate the type of correlations discussed in §1.

It is clear from the work presented here and in the references that a considerable amount of information can be revealed by NMRI methods applied to fluids permeating porous solids. Although this paper has emphasized single phase fluid-saturated states the use of the whole range of contrast mechanisms available to NMR, based on chemical shift, relaxation, diffusion and flow offers the prospect of quantitative characterization of multiphase systems in regard to local saturations, porosities, solid–fluid and fluid–fluid interactions, fluid transport and porous solid topology.

The authors thank Dr D. C. Buller, Dr A. Hardwick and Dr Z. Kalam for assistance with the selection and preparation of samples and for discussions relating to the properties of oil reservoir rocks. We thank BP Research for permission to publish this work and L. D. C. and T. A. C. thank Dr Herchel Smith for his munificent endowment.

References

Baldwin, B. A. & Yamanashi, W. S. 1988 NMR imaging of fluid dynamics in reservoir core. *Mag. Res. Imaging* **6**, 493–500.

Bendel, P. 1990 Spin-echo attentuation by diffusion in non-uniform field gradients. *J. magn. Reson.* **86**, 509–515.

Blackband, S., Mansfield, P., Barnes, J. R., Clague, A. D. H. & Rice, S. A. 1986 Discrimination of crude oil and water in sand and in bore cores with NMR imaging. *SPE Form. Eval.* **1**, 31–34.

Brownstein, K. R. & Tarr, C. E. 1979 Importance of classical diffusion in NMR studies of water in biological cells. *Phys. Rev.* A**19**, 2446–2453.

Davies, S., Kalam, M. Z., Packer, K. J. & Zelaya, F. O. 1990 Pore size distributions from NMR spin-lattice relaxation measurements of fluid-saturated porous solids. II. Applications to reservoir core samples. *J. appl. Phys.* **67**, 3170–3177.

Davies, S. & Packer, K. J. 1990 Pore size distributions from NMR spin-lattice relaxation measurements of fluid-saturated porous solids. I. Theory and simulation. *J. appl. Phys.* **67**, 3163–3169.

Edelstein, W. A., Vinegar, H. J., Tutunjian, P. N., Roemer, P. B. & Muller, O. M. 1988 NMR imaging for core analysis. *Proc. 63rd A. Tech. Conf. of Soc. Petr. Engrs*, pp. 101–112.

Hall, L. D. & Rajanayagam, V. 1987 Thin-slice chemical shift imaging of oil and water in sandstone rocks at 80 MHz. *J. magn. Reson.* **74**, 139–146.

Horsfield, M. A., Fordham, E. J., Hall, C. & Hall, L. D. 1989 ^{1}H NMR imaging studies of filtration in colloidal suspensions. *J. magn. Reson.* **81**, 593–596.

Kenyon, W. E., Day, P. I., Straley, C. & Willemsen, J. F. 1988 A three-part study of NMR longitudinal relaxation properties of water-saturated sandstones. *SPE Form. Eval.* **3**, 622–636.

Kleinberg, R. L. & Horsfield, M. A. 1990 Transverse relaxation processes in porous sedimentary rock. *J. magn. Reson.* **88**, 9–19.

Rothwell, W. P. & Vinegar, H. J. 1985 Petrophysical applications of NMR imaging. *Appl. Opt.* **24**, 3969–3972.

Vinegar, H. J. 1986 X-ray CT and NMR imaging of rocks. *J. Petr. Tech.* **38**, 257–259.

Discussion

R. F. Gordon (*Bruker Instruments Inc., Billerica, U.S.A.*). Would Professor Packer care to comment on the usefulness of ^{13}C measurements for oil core analysis in comparison with the ^{1}H measurement discussed in his talk?

K. J. Packer. I do not believe ^{13}C NMRI is going to be of much general utility because of the intrinsically low signal. No doubt special problems could be tackled by use of ^{13}C enriched fluids. For non-imaging NMR measurements, however, ^{13}C NMR can be used for direct measurement of hydrocarbons and rock carbonate. (Vinegar *et al.* 1989).

E. L. Hahn (*University of California, U.S.A.*). Regarding the assessment of molecular diffusion in structures, although Professor Packer has pointed out diffusion in one, two and three dimensions, does not this concern the diffusion problem involving reflection at boundaries so that the ordinary diffusion equation in free space is not valid? I did not sense that 'reflection' was considered.

K. J. Packer. Yes, Professor Hahn is quite correct that diffusion of fluids in a typical complex pore space will require the solution of the diffusion equation including reflection effects at the solid–fluid interfaces. This is a complex problem and one which we have been addressing recently (Callaghan *et al.* 1990).

The data, which I showed in response to the question by Dr Frahm (see below), comprised the pulsed field gradient stimulated echo attenuation behaviour of water and decane contained in a porous alumina. The echo attenuation ratios, $\ln [S(\Delta, q)/S(0)]$, are found to be nonlinear functions of the single parameter $q^2\Delta D$, where $q = \gamma g \delta$ (Packer & Zelaya 1989) and are superposable for water and decane. Over the range of q used there was no indication of a separation of the data into separate curves, this latter being the usual indication of the direct observation of the reflection effects Professor Hahn refers to (Callaghan 1984). The interpretation offered for this particular system involves the hypothesis that the confining pore space has a tube-like character. If we represent this as cylindrical, with radius a, then for times $\Delta > a^2/D$ the diffusion can be increasingly regarded as approximating to continuum diffusion in a lower-dimensionality space and the theoretical curves

shown were those for an isotropic distribution of such one- and two-dimensional paths (Callaghan 1984). For the alumina used, $a \approx 2\,\mu m$, whence Δ must be somewhat greater than *ca.* 2 ms, which was always the case. Indeed, for the results shown values as high as 1 s were used.

E. R. Andrew (*University of Florida, U.S.A.*). Many rocks contain iron, manganese and other transition metals. To what extent can this be tolerated? Are there classes of rock sample that have to be avoided in this work?

K. J. Packer. There are at least two effects which can arise from the presence of minerals containing paramagnetic species. The first is distortion of the field arising from susceptibility differences and the second is enhanced spin relaxation. Of the two main classes of reservoir rock, clean sandstones and limestones are usually the easier to image, while sandstone containing such other minerals, to which Professor Andrew refers, can be more difficult. Each material and sample is an individual case to be considered on its merits. Contrast may indeed be generated in an image through the presence of these minerals and this may be of interest.

P. A. Bottomley (*GE Research and Development Center, Schenectady, U.S.A.*). How does Professor Packer perceive the measurement provided by NMR imaging of core samples to be of benefit to oil recovery? What are the advantages of the NMR imaging measurements over conventional methods of core analysis?

K. J. Packer. I'm not sure that I can give a definitive answer to the first question. Oil recovery has many factors needing consideration. NMR imaging is a laboratory-based method (at least at present) and can be used to make spatially resolved measurements of fluid saturations/porosity, to provide direct observations of fluid transport and displacement processes, all these on real rock samples of sizes/shapes determined either by sample availability or spectrometer design limits. I believe that it is largely in the relative fluid transport behaviour and relationship to pore scale structure that NMRI is likely to have applications of the type to which Dr Bottomley refers.

I'm not clear that NMRI can be compared with conventional core analysis methods as, in the main, these latter do not address spatially resolved properties. X-ray CT would be the obvious comparison and I don't see NMRI as a direct competitor. However, non-spatially resolved NMR measurements on whole core or core plugs can offer advantage in terms of speed of measurement and the nature of the information accessible.

I. R. Young (*Hammersmith Hospital, London, U.K.*). Has Professor Packer considered looking at percolation (macroscopic flow) in parallel with the diffusion studies to which he alluded in his talk? This is by analogy with the studies on perfused flow (in parallel with diffusion) which have become a significant topic in *in vivo* MRI, and which is now the subject of substantial scientific discussion.

K. J. Packer. Yes, in fact there are very close parallels. A fluid flowing through a porous solid will have a velocity distribution characteristic of the solid pore space and the flow conditions. The velocity of any particular fluid element will also be time dependent, the nature of this depending on the starting position of the element and

PHILOSOPHICAL TRANSACTIONS OF THE ROYAL SOCIETY A MATHEMATICAL, PHYSICAL & ENGINEERING SCIENCES

its subsequent path through the pore space. Observations as a function of time (say the inter-gradient-pulse time Δ in a pulsed-field-gradient spin-echo experiment) will provide information on the velocity fluctuation spectrum.

A. N. Garroway (*Naval Research Laboratory, Washington, D.C., U.S.A.*). The free fluid index is a semi-empirical relation between NMR parameters and the amount of oil available in rock. Can NMR or NMR imaging put this relation on a sounder physical basis?

K. J. Packer. Yes, I believe it can. I'm not sure, however, that imaging is required for this. It is usually NMR measurements taken down a well bore that yield the so-called free fluid index (FFI). Laboratory-based measurements can certainly be used to give some extra interpretative confidence as to the precise meaning of such FFI values.

J. Frahm (*MPI für biophysikalische Chemie, Göttingen, F.R.G.*). (1) CHESS MRI. Has Professor Packer performed chemical shift selective imaging studies? (2) Diffusion MRI. What about diffusion imaging, e.g. using stimulated echoes exploiting their access to long diffusion time for species with long T_1 relaxation times? (3) Diffusion on micro-emulsions. Restricted diffusion might give information on pore sizes. Has he performed diffusion studies on micro-emulsions to contribute to an understanding of their structure?

K. J. Packer. (1) No, but they can and have been carried out. They usually require rather favourable properties of the rock–fluid combination. In particular the line widths must not be so large as to make the chemical shifts inaccessible. (2) The diffusion data I showed (see reply to Professor Hahn's question) were taken using the stimulated echo sequence. The general problem I refer to there, of understanding the response of the pulsed-field-gradient spin-echo method applied to fluids in porous solids, can be transposed directly to spatially resolved measurements. To that extent the imaging is just an additional detection mode. (3) No, I have not made measurements on micro-emulsions but there is quite an extensive literature of such measurements such as those from the group at Lund.

E. W. Randall (*Queen Mary and Westfield College, London, U.K.*). Professor Packer has shown the effect of variations in magnetic susceptibility on the relaxation times. There is also an effect, of course, on the image which is distorted. It appears that in his work this distortion is of no consequence but there are other cases where it is. Then one needs to use appropriate techniques to remove the susceptibility effect.

K. J. Packer. Professor Randall is quite correct and, indeed, as the susceptibility differences between fluid and rock matrix are generally larger than those encountered in medical or biological imaging samples one might expect the effects to be larger. They could well be and some of the contrast effects observed may, in part, have as a basis susceptibility effects. One point I would make, however, is that in many cases the scale of the fluid-filled porosity is much less than the image voxel dimensions. As the susceptibility induced gradients are on the scale of the pore space or even less, this means that within a given voxel there may be no net effect. It is, however, an area which requires further consideration for a full evaluation of the possible effects.

PHILOSOPHICAL TRANSACTIONS OF THE ROYAL SOCIETY A MATHEMATICAL, PHYSICAL & ENGINEERING SCIENCES

Additional references

Callaghan, P. T. 1984 Pulsed field gradient nuclear magnetic resonance as a probe of liquid state molecular organisation. *Aust. J. Phys.* **37**, 359–387.

Callaghan, P. T., MacGowan, D., Packer, K. J. & Zelaya, F. O. 1990 High-resolution q-space imaging in porous structures. *J. magn. Reson.* (In the press.)

Packer, K. J. & Zelaya, F. O. 1989 Observation of diffusion of fluids in porous solids by pulsed field gradient NMR. *Colloids Surf.* **36**, 21–227.

Vinegar, H. J., Tutunjian, P. N., Edelstein, W. A. & Roemer, P. B. 1989 Whole core analysis by ^{13}C NMR. *Proc. 64th A. Tech. Conf. of Soc. Petr. Eng.*, SPE 19590, pp. 1–5.

PHILOSOPHICAL TRANSACTIONS OF THE ROYAL SOCIETY A MATHEMATICAL, PHYSICAL & ENGINEERING SCIENCES

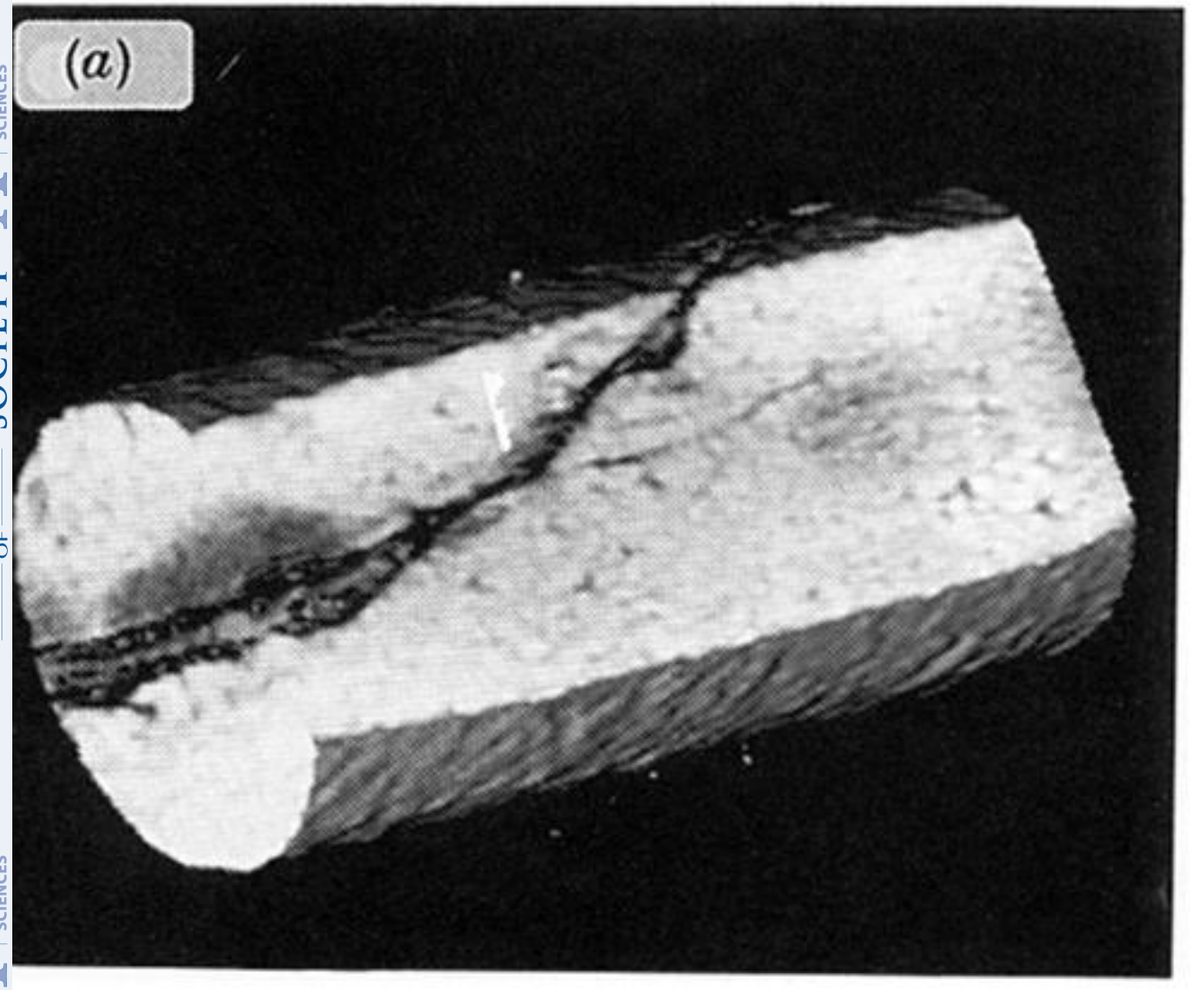

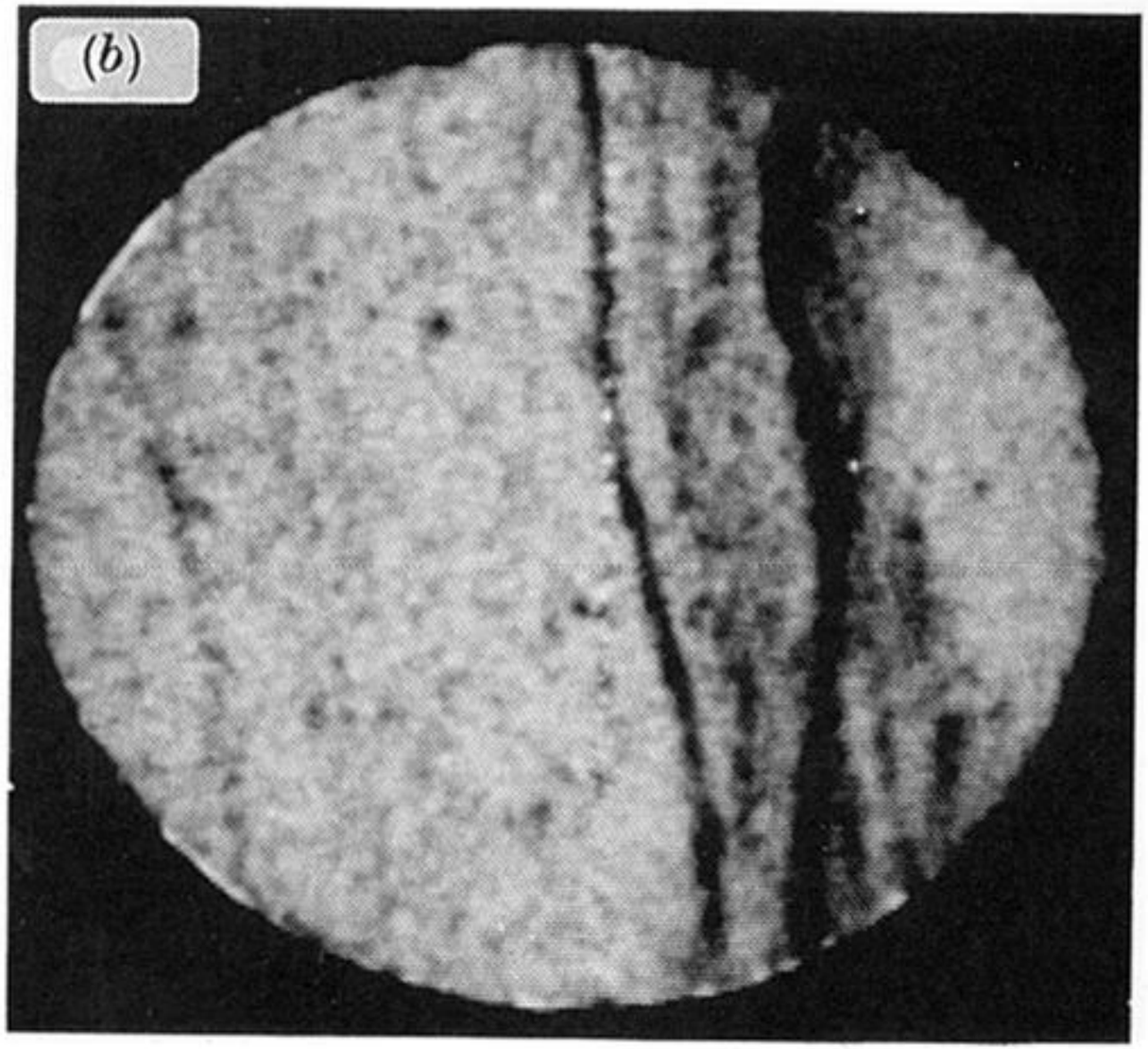

gure 1. (*a*) A ^{1}H NMR image of the brine-saturated Ninian sandstone sample. The particular image splayed was selected from a full three-dimensional data-set [$z(128)$; $y(128)$; $x(256)$; voxel size 00 μm)^3] processed using software based on ray-casting methods. The selection of cut-away ctions was made to reveal the detail of the shale band traversing the sample. A single echo was quired for each gradient combination with an echo time of 10 ms, a recycle time of 2 s and a dwell me of 6 μs. (*b*) A transverse slice-selected ^{1}H NMR image of the same sample. The in-plane solution is 200 μm × 200 μm with a slice thickness of 5 mm.

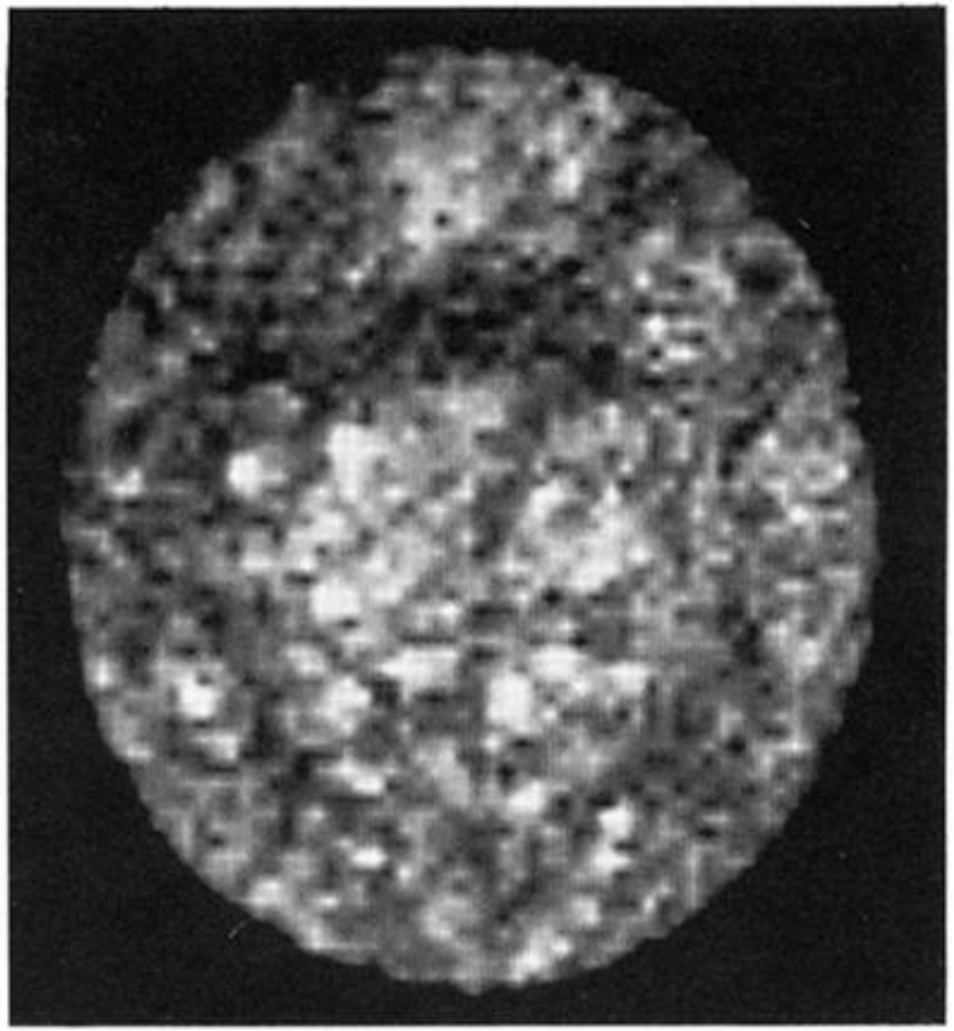

igure 2. A transverse slice-selected (5 mm) ^{1}H NMR image of the brine-saturated Dukhan nestone sample. The data were obtained using an echo time of 4.6 ms, a recycle time of 16 s and dwell time of 5 μs. The in-plane resolution is 300 μm × 300 μm.

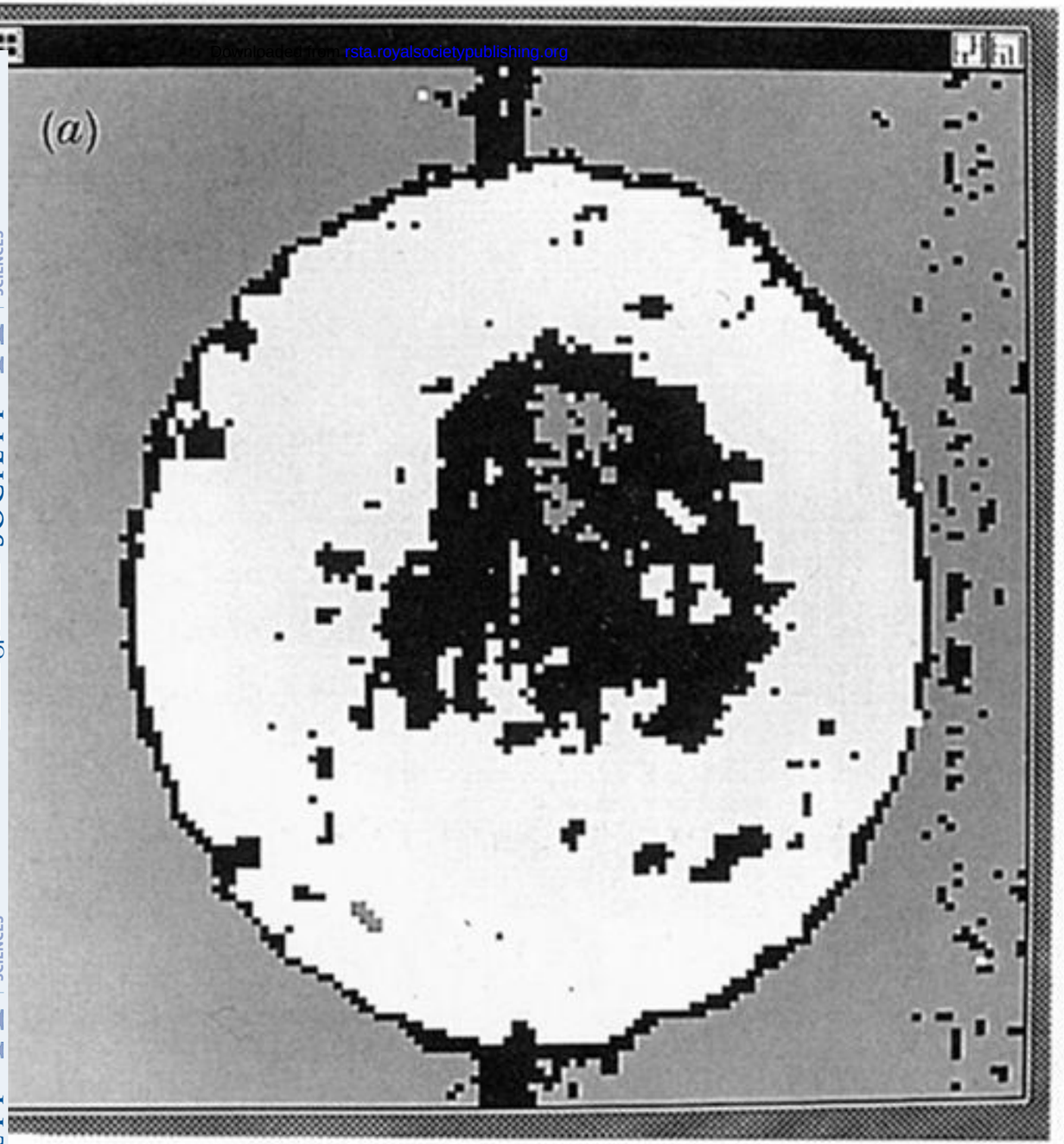

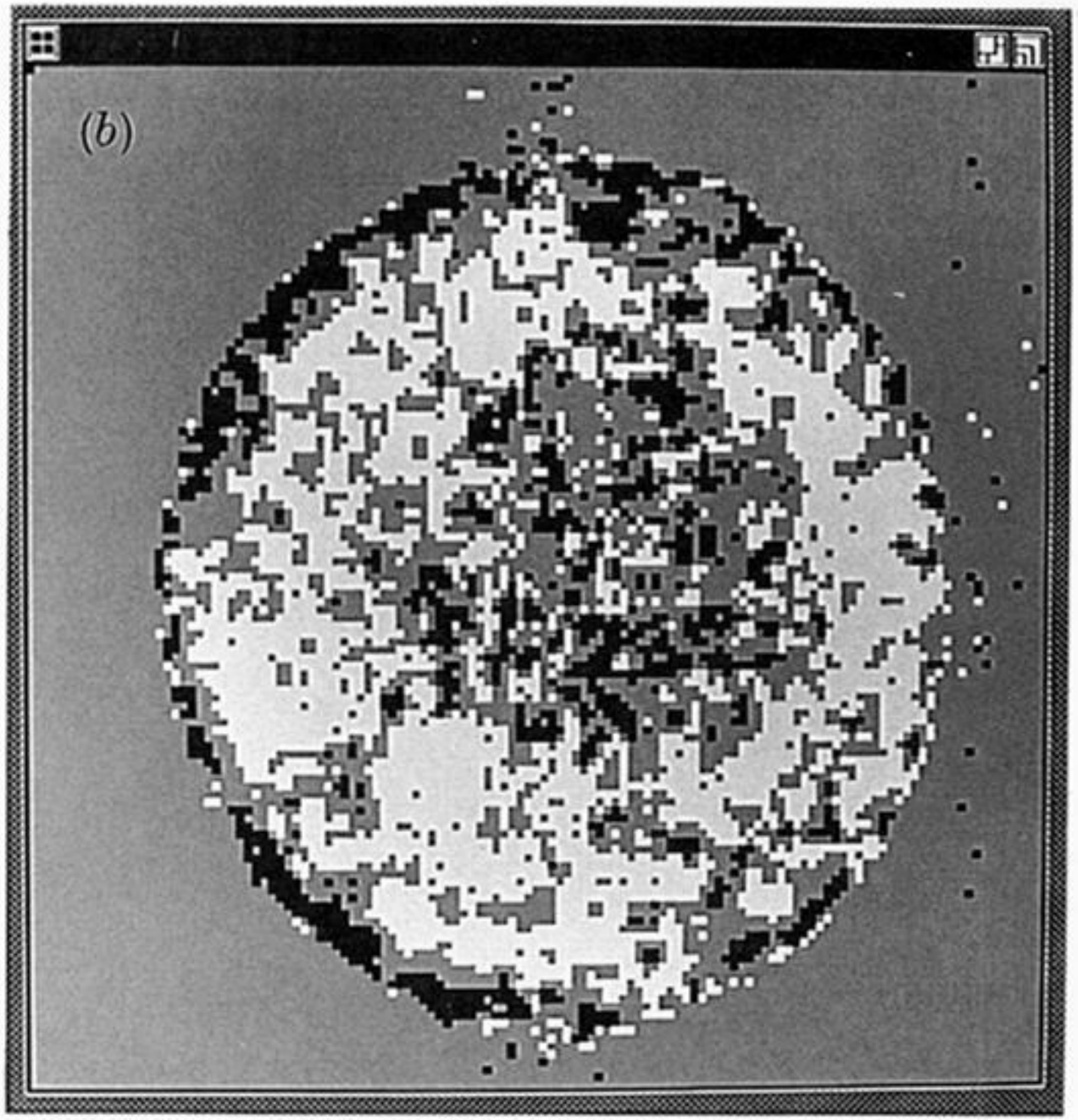

gure 4. Image displays of the Dukhan data shown in figure 3. These are two-level (black and hite) intensity and T_1 maps, (a) and (b) respectively, corresponding to the ranges identified in gure 3c, d, with black representing range A and white range B. Grey pixels are those excluded the basis that they contain below the set threshold intensity and those which were unable to be ted, for whatever reason.